AIAA JOURNAL
Vol. 49, No. 1, January 2011

Performance Variations of Leading-Edge Tubercles for Distinct Airfoil Profiles

Kristy L. Hansen,* Richard M. Kelso,† and Bassam B. Dally†
University of Adelaide, Adelaide, South Australia 5005, Australia

DOI: 10.2514/1.J050631

An experimental investigation has been undertaken to determine the influence of sinusoidal leading-edge protrusions on the performance of two NACA airfoils with different aerodynamic characteristics. Force measurements on full-span airfoils with various combinations of tubercle amplitude and wavelength reveal that when compared to the unmodified equivalent, tubercles are more beneficial for the NACA 65-021 airfoil than the NACA 0021 airfoil. It was also found that for both airfoil profiles, reducing the tubercle amplitude leads to a higher maximum lift coefficient and larger stall angle. In the poststall regime, however, the performance with larger-amplitude tubercles is more favorable. Reducing the wavelength leads to improvements in all aspects of lift performance, including maximum lift coefficient, stall angle, and poststall characteristics. Nevertheless, there is a certain point at which further reduction in wavelength has a negative impact on performance. The results also suggest that tubercles act in a manner similar to conventional vortex generators.

Nomenclature

A	=	tubercle amplitude, mm
C_d	=	drag coefficient, $2D/\rho U_\infty^2 sc$
C_L	=	lift coefficient, $2L/\rho U_\infty^2 sc$
$C_{L\,\max}$	=	maximum lift coefficient
c	=	model chord, m
D	=	drag force, N
h_{eff}	=	effective height of tubercles, $(c_{\text{peak}}\text{-}c_{\text{trough}})\sin\alpha$, mm
L	=	lift force, N
k	=	roughness height of boundary-layer trip, mm
Re	=	Reynolds number, $U_\infty c/\nu$
Re_k	=	roughness Reynolds number, $u_k k/\nu_k$
S	=	planform area, m^2
s	=	span, m
U_∞	=	freestream velocity, $m\,s^{-1}$
u_k	=	velocity of flow at roughness height, k, $m\,s^{-1}$
α	=	angle of attack
δ	=	boundary-layer thickness, mm
δ^*	=	boundary-layer displacement thickness, mm
λ	=	tubercle wavelength, mm
ν	=	dynamic viscosity, $m^2\,s^{-1}$
ν_k	=	dynamic viscosity at roughness height, k, $m^2\,s^{-1}$
ρ	=	density, $kg\,m^{-3}$

I. Introduction

TUBERCLES are leading-edge rounded protuberances that alter the flowfield around an airfoil. It has been suggested that tubercles on the humpback whale (*Megaptera novaeangliae*) flipper function as lift-enhancement devices, allowing flow to remain attached for a larger range of attack angles, thus delaying stall [1] and increasing $C_{L\,\max}$ [2]. This is considered an important characteristic for the humpback whale, which must perform tight turning maneuvers as part of its feeding ecology [3–5]. The radius of such a turn is inversely proportional to the amount of lift generated [6]; therefore, any potential increase in maximum lift coefficient would be desirable. Hence, a morphological adaptation for delaying stall would be highly beneficial for the humpback whale. Additionally, the energy expenditure required to achieve a given lift coefficient could potentially be lower, since the maximum lift coefficient for a given swimming speed would be higher. According to several researchers, the mechanism responsible for the improvement in performance is the generation of streamwise vortices, which enhance momentum exchange within the boundary layer [1,2]. Thus, there may be a strong similarity between tubercles and other vortex-generating devices currently in use, such as strakes and small delta wings [7]. Other mechanisms have also been suggested, such as the elimination of spanwise stall progression through flow compartmentalization [8].

This passive modification to the leading edge of a foil that delays stall and enables a higher maximum lift coefficient to be achieved has many potential applications for engineered lifting surfaces. Applications with Reynolds numbers similar to those of the humpback whale [2] include wind turbine blades [9], unmanned aerial vehicles [10], sailboat centerboards [8], and boat rudders [11]. Several studies on tubercles have been undertaken recently and are summarized in the following paragraphs. It can be seen that results are not in unanimous agreement about the nature of the performance improvements provided by tubercles.

Watts and Fish [12] compared the performance of a finite span (aspect ration of 2.04) NACA 63-021 airfoil with sinusoidally shaped tubercles to an unmodified airfoil using a numerical model. They reported a 4.8% increase in lift, 10.9% reduction in induced drag, and 17.6% increase in lift-to-drag ratio L/D at a 10° angle of attack. It was concluded that tubercles have a negligible effect on drag at zero angle of attack, but may incur an 11% increase in form drag at a 10° angle of attack. Images shown in Fish and Lauder [13] presented the results of an unsteady Reynolds-averaged Navier–Stokes numerical simulation with the same airfoil and angle of attack as Watts and Fish [12]. The resulting streamline images showed the formation of large streamwise vortices in the regions posterior to the troughs between tubercles. The Reynolds number was not reported for either simulation.

An experimental study undertaken by Miklosovic et al. [2] compared the lift and drag of idealized scale models (NACA 0020) of the humpback whale flipper with and without tubercles at $Re = 505,000$–$520,000$. Their results revealed a 40% increase in the stall angle, a 6% increase in the total maximum lift coefficient, and a decrease in drag in the poststall regime. The lift-to-drag ratio was larger for the airfoil with tubercles for all angles except $10° \leq \alpha \leq 12°$. These researchers [2] agreed with the analogy between tubercles and conventional vortex generators that was mentioned by Fish and Battle [1] and discussed earlier. However, van Nierop et al. [14] claimed that it is not possible for the tubercles to act as vortex

Received 29 April 2010; revision received 30 August 2010; accepted for publication 2 September 2010.

*Ph.D. Student, Mechanical Engineering Department.
†Associate Professor, Mechanical Engineering Department.

generators, since the wavelength and amplitude are much larger than the boundary-layer thickness. They propose that since tubercle peaks and troughs have different chord lengths but similar thicknesses, the pressure gradient must be higher for a trough, which causes separation to initiate in this region. According to van Nierop et al. [14], the separation behind the peaks is further delayed by a nonuniform downwash component, which leads to a reduced effective angle of attack. These researchers explained the gradual onset of global stall in relation to the variation of local stall angles with respect to spanwise location. A specific Reynolds number for this study was not reported.

Stein and Murray [15] carried out experiments for $0^\circ \leq \alpha \leq 12^\circ$ at $Re = 250,000$, using a nominally two-dimensional airfoil with sinusoidal tubercles having amplitude and spacing equal to the average values for the humpback whale. Their results showed that the modified airfoil experiences reduced lift and increased drag compared to the unmodified airfoil. A subsequent study by Murray et al. [16] used the same foils as Miklosovic et al. [2], which were modified to be positioned at various sweep angles. At $Re = 550,000$, it was found that the aerodynamic performance of an idealized model whale flipper with tubercles demonstrates superior performance in comparison to the same model with an unswept leading edge for all sweep angles under investigation. A further study by Miklosovic and Murray [8] found that the prestall lift performance of a model whale flipper is enhanced through incorporation of tubercles into the profile, whereas the prestall lift performance for a two-dimensional foil is degraded with tubercles. It must be noted that in this study [8] the Reynolds number for the model whale flipper case was $Re = 534,000$–$631,000$, while for the two-dimensional case it was almost half of that with $Re = 274,000$–$277,000$.

An experimental investigation by Johari et al. [17] compared the effect of changing the spacing and amplitude of sinusoidal tubercles on a two-dimensional NACA 63-021 airfoil. They found that for airfoils with tubercles, at $Re = 183,000$, the stall angle and maximum lift coefficient are reduced in comparison with the baseline airfoil, which is consistent with the findings in [15]. However, improvements were noted in the poststall regime in which airfoils with tubercles achieve lift coefficients as much as 50% greater than the unmodified airfoil. They also found that airfoils with smaller-amplitude tubercles perform best in terms of stall angle and $C_{L\max}$ and that varying the wavelength had negligible effects. Tuft experiments [17] showed that separation originates in the troughs between the tubercles and that the flow remains attached behind the tubercle peaks. Despite indications of an earlier separation at lower angles of attack for airfoils with tubercles, at poststall angles, the flow over the tubercle peaks is still attached when the flow over the unmodified airfoil has completely separated. Therefore, stall can be identified as the point at which the amount of lift generated begins to decrease with angle of attack, rather than when the airfoil experiences a sudden loss of lift. In reality, the modified airfoils are only partially stalled, since the flow is still attached at spanwise locations corresponding to the tubercle peaks.

Dye visualization experiments [18] using the same airfoils as [17] indicated that pairs of counter-rotating streamwise vortices are generated in the troughs between tubercles at $Re \sim 1,500$. It was suggested [18] that the formation of these vortices is a result of the spanwise flow associated with the variation in leading-edge sweep characteristic of tubercles. It was also postulated that these counter-rotating streamwise vortices may generate vortex lift similar to that observed on a delta wing [18].

The existence of streamwise vortices was supported by a computational study published by Pedro and Kobayashi [10] at $Re = 500,000$, which found that tubercles alter the vorticity distribution along the span of an idealized humpback whale flipper model at $\alpha = 15^\circ$. In comparison with an identical model with a smooth leading edge, the model with tubercles experiences increased vorticity downstream of the tubercles and a reduction in tip vortex strength at this same angle of attack. It was also observed that the extent of leading-edge separation in the tip region is reduced and there is a much more uneven trailing-edge separation line on the central third of the span in the area behind the tubercles. In some regions, separation is delayed by the presence of tubercles, which was predicted theoretically by van Nierop et al. [14]. Pedro and Kobayashi [10] attributed these characteristics to the formation of streamwise vortices associated with the presence of tubercles. In addition to increasing momentum exchange in the boundary layer, it was inferred that the tubercles also reduce the extent of spanwise flow, acting in a similar manner to wing fences.

An experimental investigation into the performance of flapping foils with tubercles was carried out by Stanway [19], using a modified scaled-down version of a whale flipper model that had been employed in a previous study [2]. The Reynolds number range was 44,000–120,000. Stanway [19] found that the foil with tubercles produces less thrust than the unmodified foil for similar power consumption. The difference in performance between the two models grows as the loading is increased. It was postulated that the vortical structures produced by the tubercles interfere with the reverse Kármán vortex street, weakening the thrust jet [19]. Another explanation was that some of the energy that would normally go into generation of the reverse Kármán vortex street is used in the creation of the streamwise vortices [19]. The researchers concluded that these findings are logical, since the humpback whale does not use its flippers as propulsors. Another important discovery in this study was that the maximum lift coefficient is reduced for all static tests (i.e. no flapping) except the one at the largest Reynolds number ($Re \sim 120,000$) [19]. This was the first example of a whale flipper model that demonstrates a reduced maximum lift for a given flow regime.

Application of tubercles to a delta wing was studied using stereoscopic particle image velocimetry by Goruney and Rockwell [20]. The researchers found that at $Re = 15,000$ and $\alpha = 25^\circ$, tubercles have a significant effect on the surface flow topology. For the smooth leading-edge profile, a negative focus of separation occurs, but for certain tubercle configurations, this can be eliminated and instead there is a positive focus of reattachment. The authors commented that the most significant change in surface topology was observed for small ratios of tubercle wavelength to amplitude.

The purpose of the experimental investigation reported in this paper is to quantify the aerodynamic benefits of sinusoidal tubercles for two different airfoils at low Reynolds numbers ($Re \sim 120,000$). The investigated airfoils have different chordwise positions of maximum thickness and are designed for different flow regimes. Thus, it was envisaged that incorporation of tubercles into these profiles would yield different results due to the variation in boundary-layer and separation characteristics. The NACA 0021 airfoil was selected, as it closely matches the cross-sectional profile of the whale flipper [2]. The maximum thickness of this profile is located at 30% of the chord. For comparison, the NACA 65-021 airfoil was used as it has a maximum thickness position further aft at 50% of the chord. It was recognized that results could be compared with those published in previous work on tubercles discussed above, which used similar airfoils. Thick airfoil sections are also used for wind turbine blades due to their softer stall characteristic [21], and thus the chosen airfoil profiles have suitable application.

The current study also aims to examine the effects of the tubercle amplitude and wavelength on airfoil performance and to identify characteristic flow patterns for airfoils with tubercles. The key dimensionless parameters investigated in this study are the ratio of amplitude to wavelength (A/λ), the ratio of the effective tubercle height to boundary-layer thickness (h_{eff}/δ), and the Reynolds number.

Another objective of the investigation is to explain the unusual occurrence of negative lift for the NACA 65-021 airfoil at low angles of attack and to determine the effect of leading-edge tubercles on this behavior. In achieving this, the effect of boundary-layer trips is also investigated.

II. Experimental Apparatus and Techniques

A. Airfoil Models

Tubercle configurations were modeled for different airfoils: NACA 0021 and NACA 65-021. The airfoils were machined from

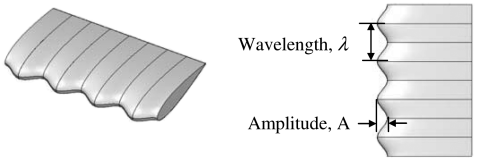

Fig. 1 Section view of airfoil with tubercles: a) 3-D view, b) plan view with characteristic dimensions.

aluminum and anodized in matte black to ensure optimum visualization of hydrogen bubbles. All airfoils are full-span models having a mean chord of $c = 70$ mm and span of $s = 495$ mm, giving a planform area of $S = 0.035$ m^2. These dimensions were chosen to minimize blockage effects and to reduce the influence of the wind-tunnel walls on the measurements. Sinusoidal tubercle configurations are illustrated in Fig. 1, and the dimensions are summarized in Table 1.

The values used here for amplitude and wavelength are close to estimates taken from data of an actual humpback whale flipper [1]. Flow visualization using the hydrogen-bubble technique was performed to observe the flowfield around the airfoil and to highlight flow-separation regions and vortex formation. Lift and drag forces for 10 different airfoils were measured in a wind tunnel.

B. Hydrogen-Bubble Visualization

Hydrogen-bubble visualization was carried out in the 0.5×0.5 m working section of a closed-return water channel manufactured in-house at the University of Adelaide. The water-channel velocity was selected to give optimum flow conditions for visualization with the hydrogen-bubble method. Thus, velocities of $U_\infty = 70$ and 84 mm/s were used, corresponding to $Re = 4370$ and 5250, respectively. This Reynolds number is substantially lower than that of wind-tunnel experiments reported in this paper. In spite of this, the large-scale vortical structures generated by the tubercles are expected to be fundamentally the same for both cases. There is some precedence for this in studies by Erm [22], where it was found that both flow patterns and normalized surface pressure measurements are very similar for Reynolds numbers differing by over an order of magnitude. Furthermore, a study by Thompson [23] found very little difference in separated vortex flow patterns around an F/A-18 aircraft for Reynolds numbers spanning four orders of magnitude.

To generate hydrogen-bubble streaklines, a low current was passed through a sinusoidally kinked platinum wire with diameter of 40 μm. The flow was illuminated using a thin light sheet ($\sim$10 mm thick) generated using an overhead projector. Images were digitally recorded via a SONY Mini-DV video camera, which was connected to a laptop computer. Footage was recorded from different orientations to highlight specific features. The side view shows the separation point; the top view shows variations in streakline spacing alluding to local pressure and velocity variations and the angled top view enables identification of vortex structures. In all cases, the flow was visualized as close as possible to the midspan location to minimize 3-D flow effects.

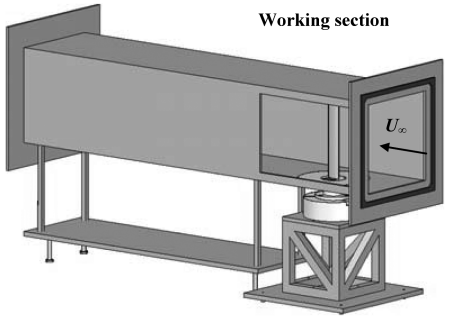

Fig. 2 Sketch of experimental setup.

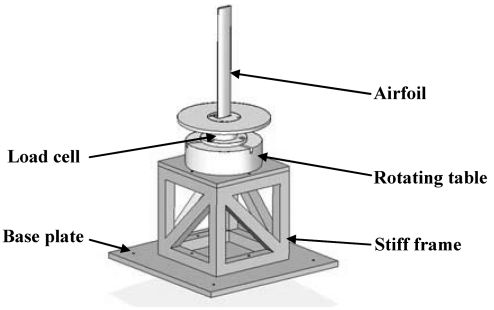

Fig. 3 Load cell arrangement.

C. Force Measurements

Force measurements were undertaken in the open section of the 0.5×0.5 m open-return wind tunnel at the University of Adelaide, which has a turbulence intensity of $\sim$0.8% and was manufactured in-house. The freestream velocity was measured using a pitot-static tube and the sampling rate was 1000 Hz. The data were averaged over 1 min and collected via a National Instruments USB-6008/6009 data acquisition system. The Reynolds number was $Re = 120,000$, based on the freestream velocity of $U_\infty = 25$ m/s and mean chord length. The working section was bolted to the exit of the wind tunnel (Fig. 2) and the top of the airfoil was located very close (3 mm) to the ceiling of the duct to minimize three-dimensional effects. This is within the range of the suggested maximum gap of $0.005 \times$ span [24]. At this streamwise location, the boundary-layer thickness based on $0.99U_\infty$ is approximately 10 mm. This value was determined experimentally using a pitot tube and measuring the local velocity at 1 mm increments, starting from the ceiling.

The foundation of the load cell consisted of a heavy steel baseplate to inhibit the effects of floor vibration and a stiff frame to minimize vibrational disturbances generated by the airflow (Fig. 3). These vibrations could potentially cause inaccuracies in the measurements. The angle of attack for the airfoil was set using a Vertex brand rotary table with an estimated uncertainty of $\pm 0.2°$. Lift, drag, and moment measurements were conducted using a six-component load cell from JR3 with external digital electronics. This was fixed to a rotary table and rotated together with the airfoil. Care was taken to ensure the airfoil was mounted as accurately as possible with regard to the

Table 1 Tubercle configurations and adopted terminology

0021 airfoils			65–021 airfoils		
Configuration	Label	A/λ ratio	Configuration	Label	A/λ ratio
0021 unmodified	0021 unmod	——	65–021 unmodified	65021 unmod	——
$A = 2$ mm (0.03c), $\lambda = 7.5$ mm (0.11c)	$A2\lambda7.5$	0.27	——	——	——
$A = 4$ mm (0.06c), $\lambda = 7.5$ mm (0.11c)	$A4\lambda7.5$	0.53	——	——	——
$A = 4$ mm (0.06c), $\lambda = 15$ mm (0.21c)	$A4\lambda5$	0.27	——	——	——
$A = 4$ mm (0.06c), $\lambda = 30$ mm (0.43c)	$A4\lambda30$	0.13	$A = 4$ mm (0.06c), $\lambda = 30$ mm (0.43c)	6$A4\lambda30$	0.13
$A = 4$ mm (0.06c), $\lambda = 60$ mm (0.86c)	$A4\lambda60$	0.07	——	——	——
$A = 8$ mm (0.11c), $\lambda = 30$ mm (0.43c)	$A8\lambda30$	0.27	$A = 8$ mm (0.11c), $\lambda = 30$ mm (0.43c)	6$A8\lambda30$	0.27

freestream flow. System calibrations showed that the load cell accuracy is within ±1%.

Results are corrected for solid blockage, wake blockage and streamline curvature according to the guidelines proposed by Barlow et al. [24]. For the highest angle of attack in the prestall regime ($\alpha = 12°$), the corrected velocity is found to be 0.6% higher, which gives an overall increase in α of 0.3%, decrease in C_L of 1.6%, and decrease in C_D of 1.3%.

The sampling period of the analog-to-digital converter was 16 ms, which ensured that at least 1000 samples were collected for each angle of attack. Because of the unsteady nature of the flow at poststall angles, the number of collected samples was increased to 3000 for these cases. The maximum standard deviation for the data set occurs poststall at $\alpha = 25°$ and is ±0.09 for C_L and ±0.03 for C_D.

Three sets of measurements were taken for each airfoil for the range of angles $-4° \leq \alpha \leq 25°$. The average results for the lift and drag coefficients for the tested airfoils were then plotted and compared. The NACA 0021 and NACA 65-021 airfoils were plotted on separate axes due to their different characteristics, but the relative influence of the tubercles for the two airfoils was compared. A conservative estimation of the uncertainty was carried out using the methods outlined by Bentley [25]. The most significant sources of error identified for the analysis were associated with the freestream velocity, load cell, and rotary table. It was found that before stall, the maximum error in C_L is ±0.09 and the maximum error in C_D is ±0.05.

III. Results

Hydrogen-bubble flow visualization images highlight the characteristic flow features for airfoils with tubercles. It was difficult to distinguish noticeable differences between the visualization results for the NACA 0021 and NACA 65-021 airfoils, and thus the focus of the reported results is the illustration of important flow features associated with tubercles as well as comparison of different tubercle configurations.

Following these results are plots of lift and drag coefficients for the modified and unmodified NACA 0021 and NACA 65-021 airfoils. A comparison will be made between the performances of these two airfoils with various tubercle configurations. In addition, an unexpected negative-lift characteristic of the NACA 65-021 airfoil at low angles of attack will be identified for both the unmodified airfoil and also the airfoils with tubercles. It will be shown that this characteristic can be eliminated through use of a boundary-layer trip and the tripped results for the NACA 65-021 airfoil will be used for comparison with the NACA 0021.

Force measurements are compared with published data, which proved to be quite scarce for these specific airfoil profiles at low Reynolds numbers. Miklosovic and Murray [8] published the lift and drag coefficients versus angle of attack for a NACA 0020 airfoil; however, the Reynolds number was approximately double the one in the present work. It can be seen in Figs. 4 and 5 that the NACA 0021 airfoil in the present study has a lower stall angle and a higher drag, which is expected for a similar airfoil profile at a lower Reynolds number. However, the general trends are very similar, particularly with regard to the abrupt stall characteristic as well as a slightly increasing lift-curve slope for angles of attack α between 5 and 8°. Comparison with the ideal lift-curve slope shows that the measured data approach this ideal slope and at one point exceed the theoretical value. The latter is attributed to experimental error.

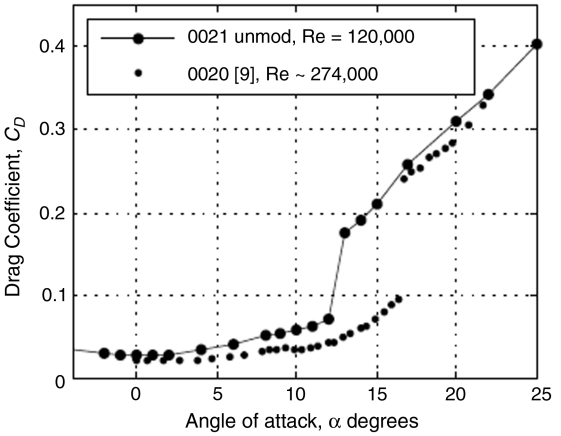

Fig. 5 Drag Coefficient vs angle of attack for NACA 0021 compared with experimental data for NACA 0020 [8].

The repeatability of the measurements can be gauged from Figs. 6 and 7, where results from three independent tests are plotted on the same set of axes for comparison. It can be seen that there is negligible difference in lift for the three runs. There is a slight variation in drag, but it is not significant, and the overall trends are the same. The same conclusions can be drawn from the fourth test (0021 foam), where the wing-tip was extended using closed-cell foam to minimize the gap between the airfoil and the test-section ceiling. This implies that end effects are not significant and the airfoils can be considered two-dimensional.

A. Visualization

Hydrogen-bubble visualization with the $A8\lambda30$ airfoil is shown in Fig. 8a and reveals that streamwise vortices are formed in the troughs between tubercles. It can also be seen in Fig. 8b that the downward turn of the flow behind a tubercle peak is greater than the behind a trough (Fig. 8c), which is consistent with calculations undertaken by van Nierop et al. [14]. This implies a greater degree of flow attachment behind a peak than behind a trough, which was also reported by Johari et al. [17]. Also, Fig. 8d indicates that the streaklines converge in the troughs and this implies that the flow is

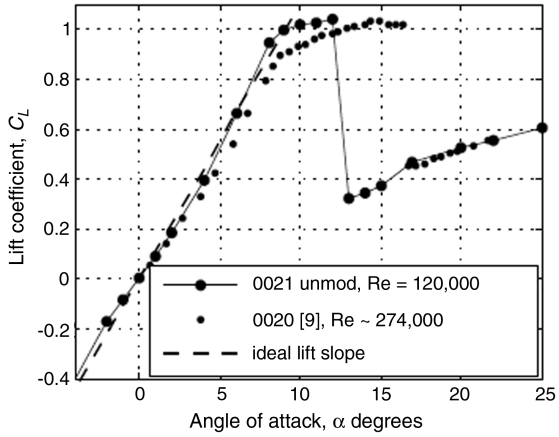

Fig. 4 Lift Coefficient vs angle of attack for NACA 0021 compared with experimental data for NACA 0020 [8].

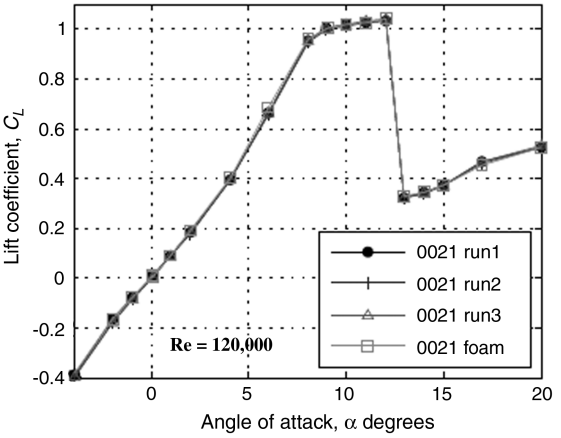

Fig. 6 Consideration of repeatability and influence of gap on lift performance of NACA 0021.

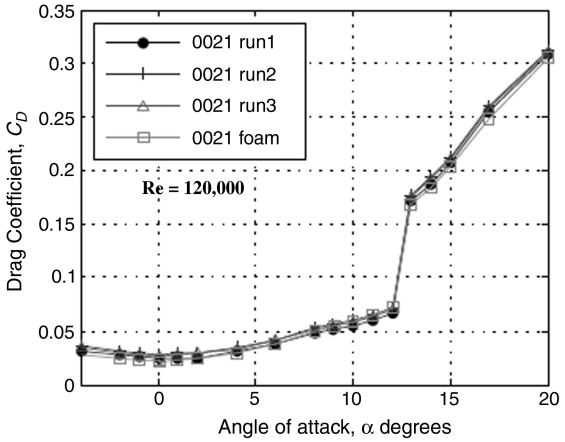

Fig. 7 Consideration of repeatability and influence of gap on drag performance of NACA 0021.

accelerated in this region. The streaklines appear to converge behind the tubercle peaks as the flow approaches the trailing edge; however, the surface flow may in fact exhibit the opposite behavior. It should be noted that Figs. 8a and 8d show streaks above the surface, not at the surface.

Figure 9 shows a comparison of the flow characteristics for various tubercle configurations as seen from an angled top view. In the case of the unmodified airfoil at $\alpha = 10°$, there is no perturbation to the streaklines as they travel along the chord of the airfoil. However, it can be seen that for all airfoils with tubercles, a three-dimensional pattern of streaklines emerges, which alludes to the presence of streamwise vortices.

For a smaller tubercle wavelength, the vortices are spaced more closely together and are therefore more likely to interact with one another. This can be seen in Figs. 9b–9d, where the onset of instability occurs further upstream with decreasing tubercle wavelength, leading to an apparent increase in turbulence. This may lead to an increased momentum exchange as well as a more uniform attachment of the flow to the airfoil surface. Considering airfoils with the same amplitude-to-wavelength ratio A/λ, and hence equivalent maximum angle of leading-edge sweep, there is a similarity between

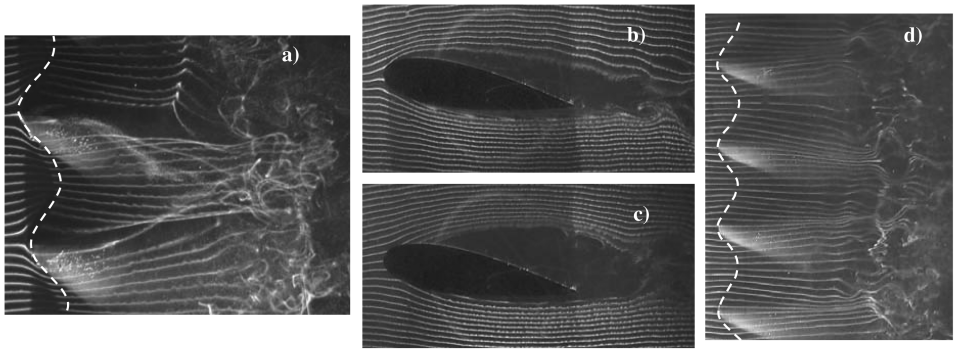

Fig. 8 Hydrogen-bubble visualization with $A8\lambda30$ airfoil at $\alpha = 10°$: a) angled top view showing streamwise vortices ($Re = 4370$), b) side view in plane of peak ($Re = 5250$), c) side view in plane of trough ($Re = 5250$), and d) top view depicting regions of acceleration ($Re = 5250$). Dashed lines show leading-edge outline.

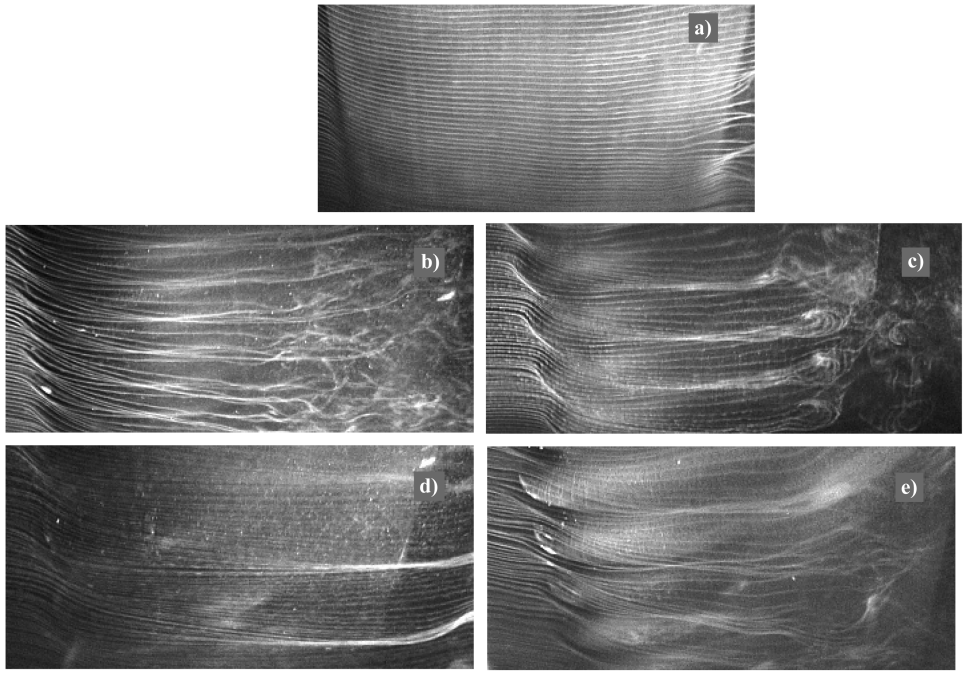

Fig. 9 Hydrogen-bubble visualization of the NACA 0021, angled top view: a) unmodified NACA 0021 airfoil, b) $A4\lambda15$, c) $A4\lambda30$, d) $A4\lambda60$. and e) $A8\lambda30$ ($Re = 5250$, and $\alpha = 10°$).

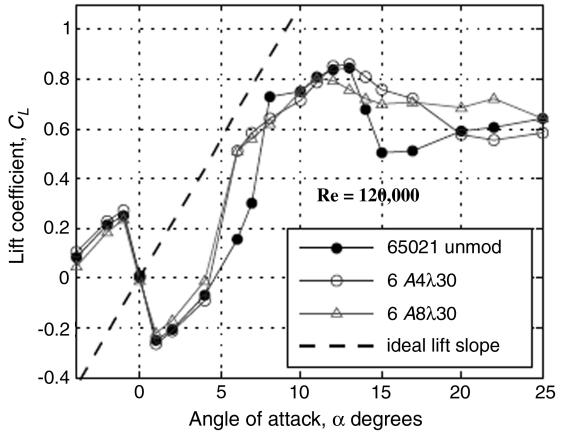

Fig. 10 Lift coefficient vs angle of attack for NACA 65-021.

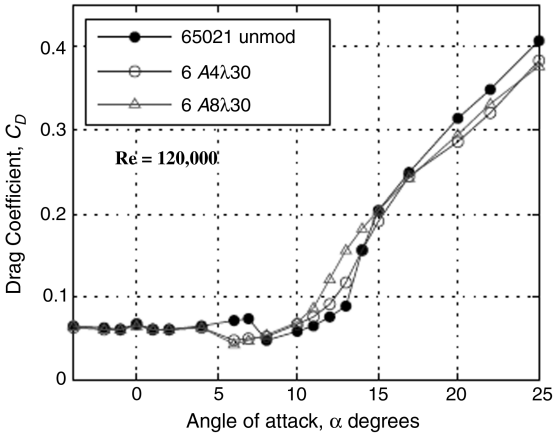

Fig. 12 Drag coefficient vs angle of attack for NACA 65-021.

Figs. 9b and 9e, with respect to the appearance of the vortex structures. This observation may be the result of a similar vortex strength for these cases, which was mentioned by Custodio [18]. In summary, it is postulated that the spacing influences the degree of mixing in the boundary layer and that the A/λ ratio may affect the vortex strength. As the spacing between tubercles is reduced, they act more like turbulence generators giving rise to more uniform boundary-layer mixing and more uniform attachment of the boundary layer near the trailing edge.

B. Negative-Lift Characteristic of NACA 65-021 Airfoil

At angles of attack between $0 \leq \alpha \leq 4°$, the NACA 65-021 airfoil produces a lift force in the opposite direction to that expected for a symmetrical airfoil at an angle of attack. Figure 10 shows that this behavior occurs for both the unmodified airfoil and the airfoils with tubercles. It can be seen that the magnitude of the negative-lift force is the same for both a clockwise and anticlockwise rotation of the airfoil, which negates the possibility that the phenomenon is due to model asymmetry as suggested by Mueller and Batill [26]. These researchers noticed the same negative-lift effect for a NACA 66_3-018 airfoil at $Re \sim 130,000$, but attributed it to surface irregularities resulting from a surface finish done by hand after milling.

Marchaj [27] also observed negative-lift generation where a comparison was made between a NACA 63-018 and a NACA 64-018 airfoil. It was found that the airfoil section with maximum thickness further aft (NACA 64-018) experienced negative-lift characteristics, whereas the other foil section had a linear lift-curve slope that passed through the origin. This author attributed the negative lift to a significant thickening of the boundary layer at the trailing edge on the top surface of the airfoil, which occurred due to the large trailing-edge angle [27]. This boundary-layer thickening leads to a larger effective curvature on the bottom surface of the foil relative to the top surface and hence negative lift.

The negative-lift behavior was ameliorated through use of a boundary-layer trip wire located at 7% of the chord from the leading edge. The height and position of the trip were optimized to give the lowest possible drag and maximum lift, while maintaining a linear relationship between C_L and α in the prestall regime. A roughness height of $k = 0.3$ mm was calculated according to the guidelines of Braslow et al. [28], using a roughness Reynolds number of $Re_k = 600$ and assuming a laminar boundary layer at the location of the roughness. This roughness height was refined through trial and error and proved to be an excellent first-order estimate, since the most successful height was $k = 0.4$ mm.

Results in Fig. 11 indicate that the negative-lift characteristic is completely eliminated and the slope of the lift curve is approximately linear. Comparison between Figs. 10 and 11 reveals that the poststall characteristics $C_{L\,\max}$ and the stall angles are almost identical. It can also be seen that the unmodified airfoil without a trip experiences an increased amount of lift at an 8° angle of attack. This could be a result of the existence of a separation bubble, which was described in Mueller and Batill [26] and this will be investigated further with surface pressure measurements. The increased lift for this particular angle of attack is not observed for the airfoil with tubercles.

Another point of interest is the difference in lift slope for the airfoils with and without tubercles (Fig. 11). Detailed experiments not reported here found that the effectiveness of the boundary-layer trip was dependent on its chordwise position. It was difficult to choose a standardized trip position for all airfoils, since those with tubercles have a variable chord length along the span. However, it was found that small variations in trip location have negligible effects on $C_{L\,\max}$. According to Soderman [29], small serrations attached to the airfoil near the leading edge are most effective when placed as close as possible to the stagnation point. However, since these

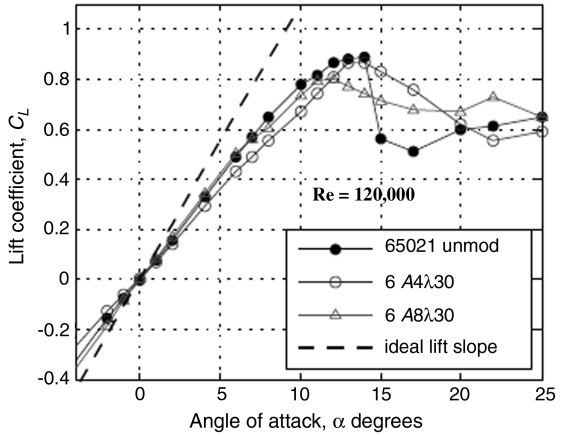

Fig. 11 Tripped lift coefficient vs angle of attack for NACA 65-021.

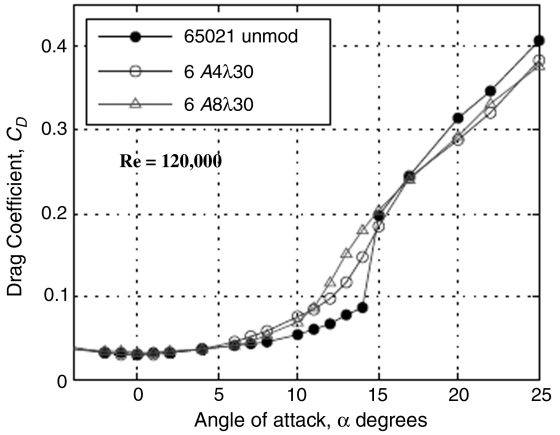

Fig. 13 Tripped drag coefficient vs angle of attack for NACA 65-021.

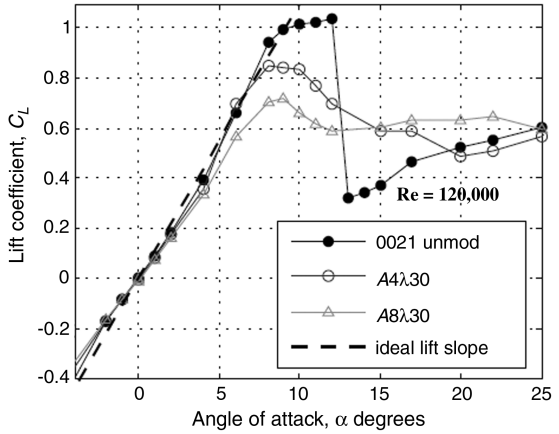

Fig. 14 Tubercle amplitude variation and the effect on lift coefficient for NACA 0021.

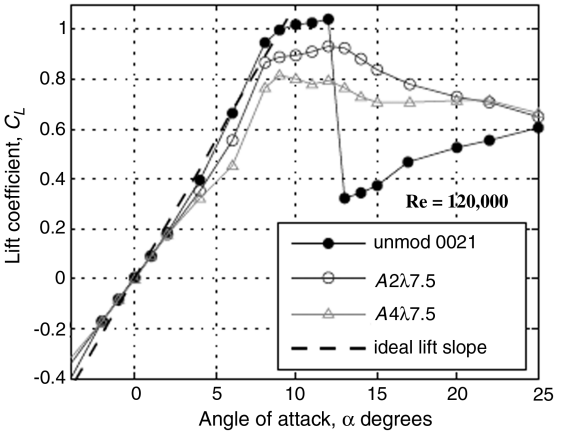

Fig. 16 Further amplitude reduction and the effect on lift coefficient for NACA 0021.

serrations produce counter-rotating vortices, it is uncertain whether this position would be most suitable for a flat trip strip. The trends found in the current experiments indicate that the positions chosen were the most effective; therefore, trip positions close to the stagnation point were not investigated.

The drag coefficient for both modified and unmodified NACA 65-021 airfoils is reduced by the presence of the boundary-layer trip for small angles of attack and is very similar for $\alpha > 10°$ (Figs. 12 and 13). This implies that at high angles of attack, the airfoil without a trip experiences an early onset of a turbulent boundary layer, which negates the effects of the trip.

C. Comparison of Airfoils and Effects of Tubercles

The lift and drag coefficients are plotted against the angle of attack for the NACA 0021 airfoils in Figs. 14 and 15. It was deemed unnecessary to use a trip for this airfoil, since the lift coefficient versus angle-of-attack curve is relatively linear. There is a slight increase in the slope of the lift plot for $5° < \alpha < 8°$, which results in a slope slightly greater than 2π; however, preliminary pressure tap measurements have found that this is not due to the presence of a separation bubble. In comparison with both the *tripped* and *untripped* NACA 65-021 airfoil (Figs. 10 and 11), the NACA 0021 airfoil produces a larger amount of lift, but stalls much more abruptly at a lower angle of attack. The drag characteristics for the two airfoils are similar and differences are associated with the fact that stall occurs at a lower angle of attack for the NACA 0021 airfoil, thus causing an earlier onset of increased drag for this airfoil.

Examining the lift coefficient plots for the two different airfoil profiles (Figs. 10, 11, and 14) reveals that the performance in the prestall regime for airfoils with tubercles is slightly more favorable for the NACA 65-021 than the NACA 0021 in comparison with the baseline airfoil. For both airfoil profiles, however, the stall characteristics are much more gradual with leading-edge tubercles and the amount of lift generated in the poststall regime is also greater.

At low angles of attack, there is very little difference in drag between the various leading-edge tubercle configurations (Figs. 12, 13, and 15). However, the width of the drag bucket is reduced for airfoils with tubercles due to the fact that these airfoils begin to stall at a lower angle of attack. For these airfoils, stall is more progressive and begins behind the troughs at a lower angle of attack. Nevertheless, as the angle of attack is increased beyond the unmodified airfoil stall point, the rate of increase in drag for the modified airfoils is lower. This leads to lower drag for airfoils with tubercles at high angles of attack. The NACA 65-021 airfoils with tubercles behave in a similar way to the NACA 0021 airfoils, except that there is a small increase in drag for $6° < \alpha < 14°$.

D. Amplitude

The effect of changing the amplitude of tubercles is the same for both airfoil profiles under investigation. Increasing the amplitude leads to a smoother stall characteristic; however, this is accompanied by a drop in the value of $C_{L\max}$ and a decrease in stall angle. Conversely, the airfoils with the smallest-amplitude tubercles achieve the highest value of $C_{L\max}$, stall angle and improved poststall characteristics in comparison with the unmodified airfoil.

The drag characteristics indicate that at low angles of attack there is very little difference in performance for the different leading-edge configurations. However, there is an increase in drag associated with the earlier onset of stall for the airfoils with larger-amplitude tubercles. In the poststall regime, the amplitude does not have a significant effect on the drag characteristics.

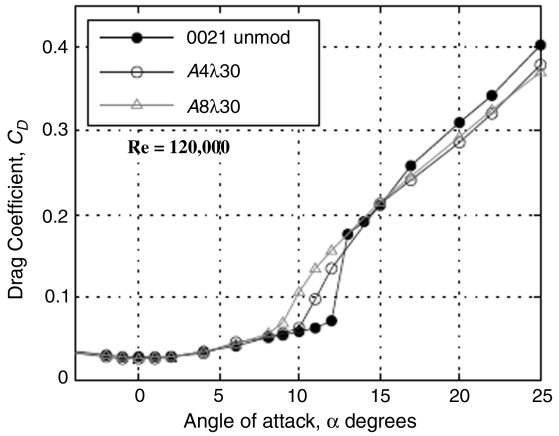

Fig. 15 Tubercle amplitude variation and the effect on drag coefficient for NACA 0021.

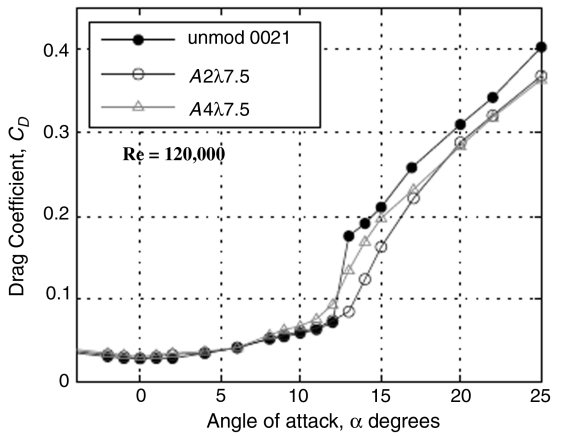

Fig. 17 Further amplitude reduction and the effect on drag coefficient for NACA 0021.

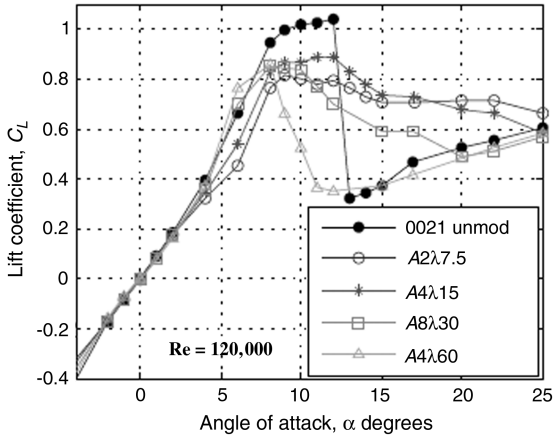

Fig. 18 Tubercle wavelength variation and the effect on lift coefficient for NACA 0021.

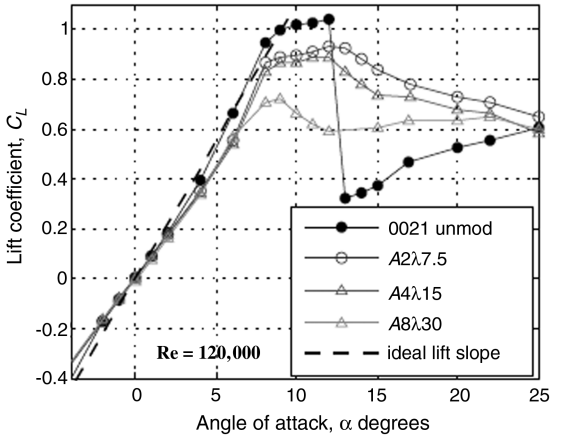

Fig. 20 Tubercle A/λ ratio and the effect on lift coefficient for NACA 0021.

Additional experiments were undertaken to determine the effect of reducing the tubercle amplitude further. Figures 16 and 17 show that both lift and drag performance are improved as the tubercle amplitude is reduced. The lift performance of the airfoil with smaller-amplitude tubercles ($A2\lambda7.5$) approaches that of the unmodified airfoil in the prestall regime. There is negligible difference in the drag coefficient for the $A2\lambda7.5$ airfoil in the prestall regime compared to the unmodified airfoil (Fig. 17). A marked improvement is observed for both the lift and drag in the poststall regime for the $A2\lambda7.5$ airfoil.

E. Wavelength

An investigation into the effects of wavelength variation on the performance of the modified airfoils was only carried out for the NACA 0021 airfoil due to budget limitations. Initial experiments suggested that as the wavelength of the tubercles is reduced, the airfoil performance improves in terms of maximum lift coefficient, stall characteristics and drag. However, it was found that for a given tubercle amplitude, there is a limitation in the improvements that can be gained through reducing the wavelength.

Figure 18 shows that the largest wavelength tubercles ($A4\lambda60$) perform poorly and in fact demonstrate no advantage in comparison with the unmodified airfoil. Reducing the wavelength by a factor of 4 ($A4\lambda15$) allows the airfoil to reach a higher angle of attack before stalling and hence a larger lift coefficient. Although this airfoil ($A4\lambda15$) achieves a lower maximum lift coefficient in comparison with the unmodified airfoil, the poststall lift characteristics are much more favorable. A further decrease in the wavelength by a factor of 2 ($A4\lambda7.5$), leads to a reduction in lift for the majority of attack angles, except $\alpha > 18°$.

As explained in the previous section, a lower drag is experienced for a larger range of angles when stall occurs at a higher angle of attack. Hence, the $A4\lambda15$ airfoil not only demonstrates favorable lift characteristics, but also shows equal or better drag performance when compared to the unmodified airfoil (Fig. 19).

The fact that there appears to be an optimal wavelength for a given amplitude of tubercles is a positive discovery in terms of manufacturing complexity. As the distance between tubercles is reduced, the cutting tool size must also decrease and the number of protrusions for a given airfoil span will increase.

F. Ratio of Amplitude-to-Wavelength (A/λ)

It was shown in Secs. III.D and III.E that for a given tubercle amplitude, there seems to be an optimum wavelength for a given airfoil profile. Thus, it is informative to compare the performance of airfoils with the same A/λ ratio. These tubercle configurations also have the same tubercle sweep angle relative to the freestream flow and as discussed in Sec. III.A, it is probable that this influences the strength of the streamwise vortices. While stall occurs at a lower angle of attack for the airfoil having larger-amplitude and wavelength tubercles, the prestall lift and drag (Fig. 20 and 21) performance are almost identical for airfoils having the same A/λ ratio. The maximum lift coefficient, largest stall angle, and lowest drag for this A/λ ratio are achieved by the airfoil with the smallest-amplitude and wavelength tubercles. This is possibly because there is a more uniform boundary-layer mixing as discussed in Sec. III.A, which leads to the greatest delay in separation.

G. Ratio of Effective Device Height to Boundary-Layer Thickness (h_{eff}/δ)

To determine the optimum tubercle amplitude for a given airfoil profile, it is suggested that the h_{eff}/δ ratio is an important parameter.

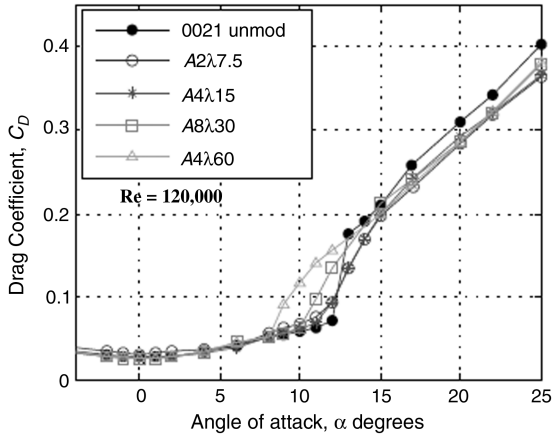

Fig. 19 Tubercle wavelength variation and the effect on drag coefficient for NACA 0021.

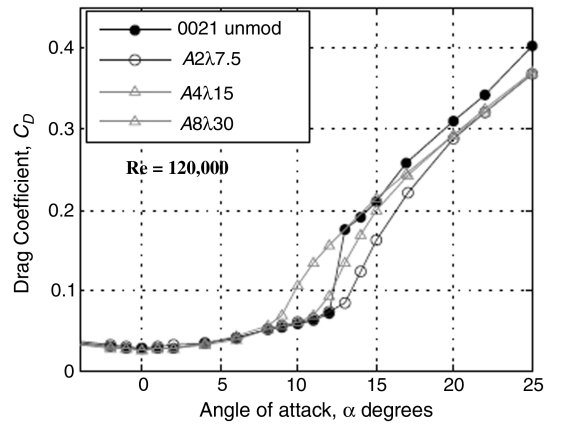

Fig. 21 Tubercle A/λ ratio and the effect on drag coefficient for NACA 0021.

Finding the value of this parameter also facilitates comparison with studies on vortex generators. The effective height h_{eff} represents the height of the device as seen by the flow and the boundary-layer displacement thickness δ^* is calculated at a chordwise distance corresponding to the tubercle amplitude using the XFOIL code [30]. The boundary-layer displacement thickness at a distance of 2 mm from the leading edge for a NACA 0021 airfoil at $Re = 120,000$ and $\alpha = 10^\circ$ is $\delta^* = 0.06$ mm. For a laminar boundary layer, the ratio of boundary-layer thickness to displacement thickness, $\delta/\delta^* \sim 2.9$ [31], giving $\delta = 0.2$ mm. For the $A2\lambda7.5$ airfoil at $\alpha = 10^\circ$, the value of $h_{\text{eff}} \sim 0.35$ mm, giving a h_{eff}/δ ratio of $\sim$0.5, which is consistent with conventional vortex generators (VGs) [32].

IV. Discussion

It is known that boundary-layer flows and separation bubbles for Reynolds numbers below 500,000 tend to be very complicated and difficult to predict [33]. The results reported here and many of those discussed in the introduction were undertaken in this low Reynolds number regime. In general, only the results at higher Reynolds numbers ($Re \geq 500,000$) showed greater performance enhancement in the prestall regime for airfoils with tubercles [2,8,10]. While all of these studies also investigated idealized model whale flippers, results published by Stanway [19] showed that for a similar whale flipper model, significantly improved lift characteristics could not be achieved at low Reynolds numbers ($44,000 < Re < 120,000$). Miklosovic and Miller [8] mentioned that the success of tubercles was related to three-dimensional effects such as spanwise stall progression. While this is a plausible benefit of tubercles, there is no conclusive evidence to suggest that at higher Reynolds numbers, two-dimensional airfoils do not demonstrate improved performance. According to Zverkov and Zanin [34], the scatter in results with regard to performance enhancement with tubercles can be understood through understanding the detailed flow pattern in the boundary layer.

Results presented in this study highlight that the effects of tubercles can vary based on the characteristics of a given airfoil profile. Comparing the NACA 0021 and NACA 65-021 airfoils reveals that the latter, which has a lower $C_{L\,\max}$ and more gradual stall, experiences negligible performance reduction in the prestall regime and performance benefits in the poststall regime ($6A4\lambda30$ configuration). It is postulated that when the position of maximum thickness is further aft, the extent of the laminar boundary layer is greater, and thus tubercles can be more beneficial. This can be explained by the fact that the rate of momentum exchange of a laminar boundary layer is much less than that of a turbulent boundary layer [27] and thus could benefit from improved momentum exchange instigated by tubercles.

The mechanism by which tubercles alter the flow characteristics over airfoils is still not completely understood. From the flow visualization results presented here and also in [18], it is clear that tubercles give rise to the formation of streamwise vortices. This idea is further supported by the fact that the force measurements for airfoils with tubercles indicate larger values of standard deviation at high angles of attack. This unsteadiness was also observed by Miklosovic and Murray [8], who suggested that it is indicative of a vortex dominated flow. It is unclear as to whether these vortices induce a type of vortex lift as suggested in the literature [8,17,18] or if they behave like vortex generators, increasing the extent of flow attachment through an augmented rate of momentum exchange within the boundary layer. It has been argued by van Nierop et al. [14] that it is implausible for tubercles to act as vortex generators, since their wavelength and amplitude are much larger than the boundary-layer thickness and that instead, they alter the pressure distribution on the wing, increasing the extent of flow attachment.

Despite this viewpoint, there are several analogies between tubercles and the counter-rotating vortex generators described in [35]. The streamwise vortices produced by VGs are found to increase in size and decrease in intensity in the streamwise direction [36], which was observed in the visualization described in Sec. III.A. In addition, the device angle has been found to be an important performance parameter for both vortex generators [32] and tubercles. In the latter case, the device angle is defined as the tubercle sweep angle, which is governed by the A/λ ratio. Similarities also exist in the flow patterns identified for VGs and tubercles, where a low-momentum region has been observed to occur between device pairs and a high-momentum region in the plane of symmetry of each device [12,36]. Adequate spacing between device pairs of VGs has been identified as a necessary condition to minimize vortex interference [37]. Since it was identified in Sec. III.E that there is a limitation to performance improvements that can be attained through reducing the wavelength between tubercles, it is postulated that the same phenomenon is responsible. Additionally, the vortex-generating mechanism would become more prominent as the angle of attack (and hence h_{eff}) increases, which is a possible explanation for the fact that the airfoils with tubercles produce more lift in the poststall regime.

This investigation also confirmed some of the trends recognized by previous researchers. For both of the airfoils tested in this study, the maximum lift coefficient is achieved with the smallest-amplitude tubercles. Similar to Johari et al. [17], the trends in the present data therefore suggest improved airfoil performance as the amplitude is decreased. The present data extend this observation further than the earlier studies, to a scale that is similar to the scale of optimum vortex generators. However, in contrast to observations made by Johari et al. [17] and van Nierop et al. [14], the wavelength has a noticeable effect on the lift performance. Reducing the wavelength improves the lift performance until a certain limit is reached, beyond which the performance is reduced for a given tubercle amplitude. Thus, it is expected that there exists an optimal amplitude-to-wavelength ratio and, when this is coupled with the most successful amplitude, the best airfoil performance characteristics can be achieved. In this study the optimum tubercle configuration was the $A2\lambda7.5$, which demonstrated both superior lift and drag in comparison to the other models with tubercles. As discussed above, it appears that the vortex generator mechanism is the best explanation for the performance enhancement provided by the tubercles. The well-documented effectiveness of small VGs with h_{eff}/δ ratios 0.2–0.5 [32] also suggests that further reduction in amplitude could improve the performance of tubercles.

For applications where the poststall lift characteristics should be optimized, it was found that relative to the maximum lift coefficient, the most gradual stall is achieved by airfoils having the largest amplitude tubercles. Reducing the wavelength also improves the poststall lift characteristics and, in fact, seems to have a greater influence, as shown by the plot for the $A2\lambda7.5$ airfoil, which has the best poststall lift performance. All except one tubercle configuration performed better than the unmodified equivalent in the poststall regime, and other researchers have also found enhanced lift characteristics in the poststall regime [2,8,17]. Thus, tubercles could be beneficial for use on foils operating near the stall point or in variable flow conditions. One such application is wind turbine blades [8]. Tubercles may also offer benefits in transitional and turbulent flow regimes, since the performance of the roughened airfoils in this study were influenced in a similar way to those that experienced natural transition.

V. Conclusions

The results indicate that the influence of tubercles varies depending on the airfoil profile under investigation. For a profile with maximum thickness located at 50% of the chord (NACA 65-021), tubercles have negligible effect on the lift performance in the prestall regime and are beneficial in the poststall regime. On the other hand, for the NACA 0021, which has maximum thickness at 30% of the chord, increased lift performance in the poststall regime comes at the expense of degraded lift performance in the prestall regime. However, it was found that through optimizing the amplitude and wavelength of the tubercles, prestall lift performance approaches the values attained by the unmodified airfoil and poststall performance is much improved.

The evidence provided by the force measurements and flow visualization suggests that the tubercles behave in a similar fashion to counter-rotating vortex generators and that the optimum tubercle amplitude and wavelength bear strong similarity to the optimum vortex generator spacing and height. The results also demonstrate that similar flow patterns occur when similar A/λ values are used.

In comparison to previous studies where tubercles improved the lift performance of the airfoils under investigation, experiments were carried out at a much lower Reynolds number. Separation characteristics are more unpredictable at such low Reynolds numbers, and the positive benefits to be attained with tubercles may be compromised. The roughened-foil results also suggest that the influence of the tubercles may be broadly similar in both laminar and turbulent flow regimes.

References

[1] Fish, F. E., and Battle, J. M., "Hydrodynamic Design of the Humpback Whale Flipper," *Journal of Morphology*, Vol. 225, 1995, pp. 51–60. doi:10.1002/jmor.1052250105

[2] Miklosovic, D. S., Murray, M. M., Howle, L. E., and Fish, F. E., "Leading Edge Tubercles Delay Stall on Humpback Whale Flippers," *Physics of Fluids*, Vol. 16, No. 5, 2004, pp. L39–L42. doi:10.1063/1.1688341

[3] Edel, R. K., and Winn, H. E., "Observations on Underwater Locomotion and Flipper Movement of the Humpback Whale *Megaptera novaeangliae*," *Marine Biology*, Vol. 48, No. 3, 1978, pp. 279–287. doi:10.1007/BF00397155

[4] Jurasz, C. M., and Jurasz, V. P., "Feeding Modes of the Humpback Whale, *Megaptera novaeangliae*, in Southeast Alaska," *Scientific Reports of the Whales Research Institute*, Vol. 31, 1979, pp. 69–83.

[5] Hain, J. H. W., Carter, G. R., Kraus, S. D., Mayo, C. A., and Winn, H. E., "Feeding Behaviour of the Humpback Whale, *Megaptera novaeangliae*, in the Western North Atlantic," *Fishery Bulletin*, Vol. 80, 1982, pp. 259–268.

[6] Weihs, D., "Effects of Swimming Path Curvature on the Energetics of Fish Swimming," *Fishery Bulletin*, Vol. 79, 1981, pp. 171–176.

[7] Fish, F. E., Howle, L. E., and Murray, M. M., "Hydrodynamic Flow Control in Marine Mammals," *Integrative and Comparative Biology*, Vol. 48, 2008, pp. 788–800. doi:10.1093/icb/icn029

[8] Miklosovic, D. S., and Murray, M. M., "Experimental Evaluation of Sinusoidal Leading Edges," *Journal of Aircraft*, Vol. 44, 2007, pp. 1404–1407. doi:10.2514/1.30303

[9] Lissaman, P. B. S., "Low-Reynolds-Number Airfoils," *Annual Review of Fluid Mechanics*, Vol. 15, 1983, pp. 223–239. doi:10.1146/annurev.fl.15.010183.001255

[10] Pedro, H. T. C., and Kobayashi, M. H., "Numerical Study of Stall Delay on Humpback Whale Flippers," 46th AIAA Aerospace Sciences Meeting and Exhibit, Reno, NV, AIAA Paper 2008-0584, 7–10 Jan. 2008.

[11] Weber, P. W., Howe, L. E., and Murray, M. M., "Lift, Drag and Cavitation Onset On Rudders With Leading Edge Tubercles," *Marine technology*, Vol. 47, No. 1, Jan. 2010, pp. 27–36.

[12] Watts, P., and Fish, F. E., "The Influence of Passive, Leading Edge Tubercles on Wing Performance," *Unmanned Untethered Submersible Technology (UUST)*, Autonomous Undersea Systems Inst., Lee, NH, Aug. 2001.

[13] Fish, F. E., and Lauder, G. V., "Passive and Active Flow Control by Swimming Fishes and Mammals," *Annual Review of Fluid Mechanics*, Vol. 38, 2006, pp. 193–224. doi:10.1146/annurev.fluid.38.050304.092201

[14] van Nierop, E., Alben, S., and Brenner, M. P., "How Bumps on Whale Flippers Delay Stall: an Aerodynamic Model," *Physical Review Letters*, Vol. 100, Feb. 2008, Paper 054502. doi:10.1103/PhysRevLett.100.054502

[15] Stein, B., and Murray, M. M., "Stall Mechanism Analysis of Humpback Whale Flipper Models," *Unmanned Untethered Submersible Technology (UUST)*, Autonomous Undersea Systems Inst., Lee, NH, Aug. 2005.

[16] Murray, M. M., Miklosovic, D. S., Fish, F. E., and Howle, L. E., "Effects of Leading Edge Tubercles on a Representative Whale Flipper Model at Various Sweep Angles," *Unmanned Untethered Submersible Technology (UUST)*, Autonomous Undersea Systems Inst., Lee, NH, Aug. 2005.

[17] Johari, H., Henoch, C., Custodio, D., and Levshin, A., "Effects of Leading-Edge Protuberances on Airfoil Performance," *AIAA Journal*, Vol. 45, No. 11, Nov. 2007, pp. 2634–2642. doi:10.2514/1.28497

[18] Custodio, D., "The Effect of Humpback Whale-Like Leading Edge Protuberances on Hydrofoil Performance," M.S. Thesis, Worcester Polytechnic Inst., Worcester, MA, 2007.

[19] Stanway, M. J., "Hydrodynamic Effects of Leading-Edge Tubercles on Control Surfaces and in Flapping Foil Propulsion," M.S. Thesis, Massachusetts Inst. of Technology, Cambridge, MA, 2008.

[20] Goruney, T., and Rockwell, D., "Flow Past a Delta Wing with a Sinusoidal Leading Edge: Near-Surface Topology and Flow Structure," *Experiments in Fluids*, Vol. 47, 2009, pp. 321–331. doi:10.1007/s00348-009-0666-x

[21] Hansen, M. O., *Aerodynamics of Wind Turbines*, James & James, London, 2000, p. 79.

[22] Erm, L. P., "Measurement of Flow-Induced Pressures on the Surface of a Model in a Flow Visualization Water Tunnel," *Experiments in Fluids*, Vol. 35, 2003, pp. 533–540. doi:10.1007/s00348-003-0667-0

[23] Thompson, D. H., "Water Tunnel Flow Visualisation of Vortex Breakdown over the F/A-18," Defence Science and Technology Organisation, Aeronautical Research Lab., Flight Mechanics Rept. 179, Melbourne, Australia, 1990.

[24] Barlow, J. B., Rae, W. H., Jr., and Pope, A., *Low-Speed Wind Tunnel Testing*, 3rd ed., Wiley, New York, 1999.

[25] Bentley, R. E., "Uncertainty in Measurement: The ISO Guide," National Measurement Inst., Sydney, Australia, 2005.

[26] Mueller, T. J., and Batill, S. M., "Experimental Studies of Separation on a Two-Dimensional Airfoil at Low Reynolds Numbers," *AIAA Journal*, Vol. 20, No. 4, April 1982, pp. 457–463. doi:10.2514/3.51095

[27] Marchaj, C. A., *Aero-Hydrodynamics of Sailing*, Granada, London, 1979, pp. 222–226, 230–235.

[28] Braslow, A. L., Hicks, R. M., and Harris, R. V, Jr., "Use of Grit-Type Boundary-Layer-Transition Trips on Wind-Tunnel Models," NASA TN D-3579, 1966.

[29] Soderman, P. T., "Aerodynamic Effects of Leading-Edge Serrations on a Two-Dimensional Airfoil," NASA TM X-2643, 1972.

[30] Drela, M., and Youngren, H., "XFOIL 6.94 User Guide," Department of Aeronautical and Astronautical Engineering, Massachusetts Inst. of Technology, Cambridge, MA, Dec. 2001.

[31] Blasius, H., "Grenzschichten in Flüssigkeiten mit kleiner Reibung," *Zeitschrift für Mathematik und Physik*, Vol. 56, 1908, pp. 1–37; also "The Boundary Layers in Fluids with Little Friction," NACA TM-1256, Feb. 1950 (in English).

[32] Lin, J. C., "Research on Low-Profile Vortex Generators to Control Boundary-Layer Separation," *Progress in Aerospace Sciences*, Vol. 38, 2002, pp. 389–420. doi:10.1016/S0376-0421(02)00010-6

[33] Simons, M., *Model Aircraft Aerodynamics*, Special Interest Model Books, Dorset, England, U.K., 2002, p. 112.

[34] Zverkov, I., and Zanin, B., "Disturbances Growth in Boundary Layers on Classical and Wavy Surface Wings," *AIAA Journal*, Vol. 46, No. 12, 2008, pp. 3149–3158. doi:10.2514/1.37562

[35] Kermode, A. C., *Mechanics of Flight*, Pitman, London, 1972, pp. 350–352.

[36] Godard, G., and Stanislas, M., "Control of a Decelerating Boundary Layer. Part 1: Optimisation of Passive Vortex Generators," *Aerospace Science and Technology*, Vol. 10, 2006, pp. 181–191. doi:10.1016/j.ast.2005.11.007

[37] Ashill, P. R., Fulker, J. L., and Hackett, K. C., "Studies of Flows Induced by Sub Boundary Layer Vortex Generators (SBVGs)," 1st AIAA Flow Control Conference, AIAA Paper 2002-3162, St. Louis, MO, June 2002.

F. Coton
Associate Editor